Scientia Pharmaceutica

Article

Evidence of Hyperglycemic Levels Improving the Binding Capacity between Human Serum Albumin and the Antihypertensive Drug Hydrochlorothiazide

Marilia Amável Gomes Soares [1], Franklin Souza-Silva [2,3], Carlos Roberto Alves [4], Leonardo Vazquez [5], Talita Stelling de Araujo [6], Carlos Serpa [7] and Otávio Augusto Chaves [7,8,*]

1 Comissão Brasileira de Energia Nuclear, Instituto de Engenharia Nuclear, Laboratório de Nanoradiofármacos e Síntese de Novos Radiofármacos, Rio de Janeiro 21941-906, Brazil; marilia.agsoares@gmail.com
2 Centro de Desenvolvimento Tecnológico em Saúde, Fundação Oswaldo Cruz, Avenida Brasil 4365, Manguinhos, Rio de Janeiro 21040-900, Brazil; franklin.souza@fiocruz.br
3 Faculdade de Biologia e Ciências da Saúde, Universidade Iguaçu, Avenida Abílio Augusto Távora 2134, Dom Rodrigo, Nova Iguaçu 26260-045, Brazil
4 Laboratório de Biologia Molecular e Doenças Endêmicas, Instituto Oswaldo Cruz, Fundação Oswaldo Cruz, Avenida Brasil 4365, Manguinhos, Rio de Janeiro 21040-900, Brazil; calves@ioc.fiocruz.br
5 Programa de Biologia Estrutural, Laboratório Estrutural e Regulação de Proteínas e ATPases, Instituto de Bioquímica Médica Leopoldo de Meis, Universidade Federal do Rio de Janeiro, Rio de Janeiro 21941-902, Brazil; leonardo_vazquez@hotmail.com
6 Centro Nacional de Biologia Estrutural e Bioimagem (CENABIO), Universidade Federal do Rio de Janeiro, Rio de Janeiro 21941-902, Brazil; tsaraujo@bioqmed.ufrj.br
7 Departamento de Química, Centro de Química de Coimbra-Institute of Molecular Sciences (CQC-IMS), Universidade de Coimbra, Rua Larga, 3004-535 Coimbra, Portugal; serpasoa@ci.uc.pt
8 Laboratório de Imunofarmacologia, Centro de Pesquisa, Inovação e Vigilância em COVID-19 e Emergências Sanitárias (CPIV), Instituto Oswaldo Cruz, Fundação Oswaldo Cruz, Rio de Janeiro 21040-361, Brazil
* Correspondence: otavioaugustochaves@gmail.com

Citation: Soares, M.A.G.; Souza-Silva, F.; Alves, C.R.; Vazquez, L.; de Araujo, T.S.; Serpa, C.; Chaves, O.A. Evidence of Hyperglycemic Levels Improving the Binding Capacity between Human Serum Albumin and the Antihypertensive Drug Hydrochlorothiazide. *Sci. Pharm.* **2024**, *92*, 32. https://doi.org/10.3390/scipharm92020032

Academic Editor: William A. Donaldson

Received: 8 April 2024
Revised: 26 May 2024
Accepted: 28 May 2024
Published: 7 June 2024

Copyright: © 2024 by the authors. Licensee MDPI, Basel, Switzerland. This article is an open access article distributed under the terms and conditions of the Creative Commons Attribution (CC BY) license (https://creativecommons.org/licenses/by/4.0/).

Abstract: Cardiovascular diseases (CVDs), especially arterial hypertension, stand as prominent contributors to global mortality. Regrettably, individuals with diabetes encounter a two-fold increase in the risk of mortality associated with CVDs. Hydrochlorothiazide (HCTZ) represents a primary intervention for hypertension, particularly in diabetic patients. Nevertheless, there has not yet been a comprehensive assessment of the biophysical characteristics regarding the impact of glucose levels on its binding affinity with human serum albumin (HSA). Thus, the present work reports the interactive profile of HSA/HCTZ in nonglycemic, normoglycemic (80 mg/dL), and hyperglycemic (320 mg/dL) conditions by time-resolved fluorescence, saturation transfer difference–nuclear magnetic resonance (STD-NMR), and surface plasmon resonance (SPR). There was a moderate ground state association of HSA/HCTZ with subdomain IIA that was affected in the presence of different glucose levels. The hyperglycemic condition decreased the binding affinity of HCTZ to subdomain IIA and increased the possibility of subdomain IB also being considered as a secondary binding site due to cooperativity and/or alterations in the protein's structure. Overall, the glucose level under hyperglycemic conditions led to the cavities being more likely to receive more ligands, offering insights into the necessity of glucose control in the human bloodstream to not impact the residence time (pharmacokinetic profile) and pharmacotherapeutic potential of HCTZ.

Keywords: biophysical characterization; diabetes mellitus; pharmacokinetic; STD-NMR; time-resolved fluorescence; surface plasmon resonance

1. Introduction

Cardiovascular diseases (CVDs) are the main causes of death, and among them, the most representative is arterial hypertension [1–3], e.g., according to studies by the Global Burden of Disease, in 2017, among the 17 million deaths from CVDs, arterial hypertension

was responsible for at least 51% of them. Overall, arterial hypertension already affects at least 600 million people worldwide, with an estimated increase of 60% in cases until 2025 [4–6]. The risk of death from CVDs increases in diabetic patients, especially if there is another comorbidity [7–9]. As the main cause of morbidity in patients with diabetes mellitus (DM) is due to macro- and microvascular complications, the risk of arterial hypertension is high, and blood pressure control is a major challenge for these patients [10,11].

In this sense, several classes of drugs have been used in the treatment of hypertension in patients with DM, e.g., beta-blockers, calcium channel blockers, and thiazide diuretics [12,13]. Hydrochlorothiazide (HCTZ; Figure 1) belongs to the group of thiazide diuretics and is the drug of first choice for the initial treatment of hypertensive patients, reducing blood pressure. HCTZ is mainly used daily in low doses (<25 mg/day). According to the recent 2023 European Society of Hypertension (ESH) guidelines, as well as the previous 2018 European Society of Cardiology (ESC) and ESH guidelines on hypertension, both thiazide and thiazide-like diuretics are indicated as drugs to be used in combination therapies for the first-line therapy of hypertension [14,15].

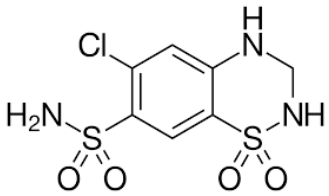


Figure 1. Chemical structure of hydrochlorothiazide (HCTZ).

The interaction of a drug with blood components influences its bioavailability and can affect the functions of various endogenous and exogenous compounds [16–19]. Human serum albumin (HSA) is the main transport protein in the human bloodstream, constituting 60% of the total globular proteins, playing an effective role in the balance of the plasma concentration of drugs and their metabolites, influencing their absorption, distribution, elimination, and clinical effects [20–25]. From a structural point of view, HSA contains 585 amino acid residues (with a molecular weight of 66.5 kDa) distributed in three main domains (I, II, and III). These domains are subdivided into A and B, having a helical shape, and are extensively cross-linked through disulfide bonds. The tryptophan residue (Trp) at position 214 in subdomain IIA is primarily responsible for the intrinsic fluorescence of HSA [26,27]. Recently, a report on the interactive profile between HSA and the monosaccharides fructose, glucose, and arabinose [20] indicated a spontaneous and weak binding with subdomain IIA. Additionally, the spectroscopic and in silico results showed that the monosaccharides might cause functional perturbation in the binding capacity of albumin to endogenous and exogenous compounds, highlighting the importance of characterizing the binding affinity of commercial drugs in normoglycemic and hyperglycemic conditions [20,28]. Glucose levels in a normoglycemic condition are in the range of 70–100 mg/dL, while an increased risk for diabetes is considered when glucose levels are in the 100–125 mg/dL range, and glucose levels higher than 200 mg/dL indicate a hyperglycemic condition. For this reason, there are some reports on the biophysical characterization of albumin-binding drugs at 80 and 320 mg/dL glucose levels under in vitro normoglycemic and hyperglycemic conditions [20,29].

Previously, Soares and coworkers [30] reported a preliminary interactive profile between HSA and HCTZ in nonglycemic, normoglycemic (80 mg/dL), and hyperglycemic (320 mg/dL) conditions via absorption and steady-state fluorescence techniques. The spectroscopic data indicated high glucose concentrations might perturb the available binding sites due to the albumin's conformational change, making the binding of HCTZ in the vicinity of the Trp-214 residue difficult. These results indicated that glycemic control is required to obtain an appropriate treatment with HCTZ. However, we did not identify the main fluorescence quenching mechanism, which is extremely important to verify the best mathematical approach to determine the binding affinity. It is also important to mention that there

are more sensitive techniques than absorption and steady-state fluorescence to determine the binding affinity [31], e.g., saturation transfer difference (STD) is the most encountered ligand-detecting nuclear magnetic resonance (NMR) method for small-molecule target studies, while surface plasmon resonance (SPR) is a very sensitive technique to explore specific binding sites [32]. Thus, to continue the binding characterization of albumin/HCTZ and better clarify the effect of glucose levels on the binding affinity, the present work reports the interactive profile of HSA/HCTZ in nonglycemic, normoglycemic (80 mg/dL), and hyperglycemic (320 mg/dL; extreme case) conditions using time-resolved fluorescence combined with the STD-NMR and SPR techniques. Overall, understanding the influence of glucose on the HSA/HCTZ association will provide valuable insights into the structural dynamics and binding specificity, emphasizing the importance of comprehensively exploring molecular interactions in complex physiological environments.

2. Materials and Methods

2.1. Chemicals

Commercially available HSA (purity $\geq$ 99%), *D*-(+)-glucose, phosphate buffer solution (PBS; pH 7.4), digitoxin, warfarin, Ludox®, and HCTZ were purchased from the Merck KGaA company (Darmstadt, Germany) and used without further purification. Ethanolamide and the amine-coupling agents 1-ethyl-3-(3-dimethylaminopropyl)carbodiimide (EDC) and *N*-hydroxysuccinimide (NHS) were purchased from Cytiva/GE Healthcare (Piscataway, NJ, USA), while the sensor chip with a matrix of carboxymethylated dextran covalently attached to a gold surface (COOH5) was acquired from FortéBio—Sartorius BioAnalytical Instruments (New York, NY, USA). Milli-Q water was obtained with a Direct System QUV3-Millipore (Darmstadt, Germany) at 24.1 °C and 18.2 mΩ. The concentration of the stock solutions of albumin was confirmed by the UV absorption, using a molar absorptivity (ε) of 35,700 M^{-1} cm^{-1} at 280 nm in the PBS [26].

2.2. Time-Resolved Fluorescence Measurements

The spectrofluorometer model FL920 CD (Edinburgh Instruments Ltd., Livingston, UK) was used to obtain the time-resolved fluorescence decays (λ_{exc} = 280 $\pm$ 10 nm) at room temperature (298 K). The corresponding decays in nonglycemic conditions were obtained for 10 μM of HSA solution (3 mL in PBS) without and with HCTZ at a concentration of 13.4 μM. In normoglycemic and hyperglycemic conditions, the fluorescence decays for HSA (10 μM) in the presence of 80 and 320 mg/dL of glucose were recorded, respectively, before and upon the addition of 13.4 μM of HCTZ. The instrument response function (IRF) was obtained for a mixture of titanium dioxide (TiO_2), water, and glycerol (Ludox® dispersion). The fluorescence decay lifetimes were analyzed using deconvolution software provided by Edinburgh Instruments. The average fluorescence lifetime ($\tau_{average}$) was determined following Equation (1):

$$\tau_{average} = \frac{\sum A_i \, \tau_i^2}{\sum A_i \, \tau_i} \quad (1)$$

where τ_i is the fluorescence lifetime, and A_i is the pre-exponential factor.

2.3. STD-NMR Measurements

The STD-NMR experiments were performed at 298 K with a Bruker Avance III spectrometer (Bruker BioSpin, Rheinstetten, Germany) operating at a ^1H frequency of 600 MHz equipped with a triple-resonance *Z*-axis gradient 5 mm probe. The D_2O signal was used as the lock signal for the instrument, while tetramethylsilane (TMS) was used as an internal reference. The HSA sample used for these experiments was prepared in PBS. The samples were prepared with a 100-fold excess of HCTZ (2 mM) vs. protein, at 20 μM. The experiments performed in the presence of glucose (at 2 mM, 10 mM, and 20 mM) were acquired in the same experimental conditions. The on-resonance spectrum was obtained with the saturation of protein signals at 0.78 ppm and the off-resonance spectrum at −10 ppm, using the Bruker standard parameters (STDDIFFGP.3). A spin-lock filter of 40 ms was used to

suppress protein signals. A saturation time build-up curve was obtained to evaluate if an accumulation of saturated ligand molecules was occurring. The saturation times used were 0.5, 1.0, 1.5, 2.0, 2.5, 3.0, 3.5, and 4.0 s with a recycling delay of 4.0 s. The STD amplification factor (A_{STD}) values were determined using the mathematical approximation reported in the literature [33]. The relative STD percentages were obtained using 2.5 s for saturation. The highest intensity of A_{STD} was set to 100%, and all other STD signals were calculated relative to this.

2.4. Surface Plasmon Resonance (SPR) Measurements

The SPR experiments were performed with an optical biosensor transduction SensíQ® Pioneer FortéBio—Sartorius BioAnalytical Instruments (New York, NY, USA) at room temperature (298 K). The samples of protein were incubated (for 30 min at 298 K) with a 10 mM acetate buffer (pH 4.5), and then the protein immobilization was performed as previously described in [34,35] with modifications. Briefly, a COOH5 sensor chip was functionalized with HSA (100 µg) using the EDC/NHS coupling method. The COOH5 covering with HSA was performed with running PBS (pH 7.4) in sequential steps at a continuous flow rate: (i) injection of 50 µL of the mixture (1:1; 0.4 M EDC and 0.1 M NHS) for 2 min at 50 µL/min; (ii) injection of HSA (100 µg) for 5 min at 50 µL/min; and (iii) injection of 150 µL of 100 mM ethanolamine at 20 µL/min.

Binding assays were performed with 50 µL injections of different concentrations (0.21–26.8 µM) of HCTZ and site markers (warfarin and digitoxin) at a continuous flow rate (50 µL/min) to access the bioavailability of HSA binding sites after immobilization on the sensor chip. Calibration curves were plotted for each ligand and then competition assays were performed with combinations of the concentration of these ligands based on the affinity constant (K_D) obtained for each. Subsequently, the influence of a glucose-enriched environment (80 mg/dL and 320 mg/dL) on HSA binding to HCTZ was evaluated by the new K_D value obtained, maintaining an equimolecular rate concentration. Subsequently, the binding of HCTZ (13.4–209 µM) to HSA was evaluated in a glucose-enriched environment, maintaining a stoichiometric ratio with glucose, based on the amount of HSA immobilized per sensor chip surface area (1.24 ng in 0.155 mm^2). After binding pulses with each ligand concentration, the sensor chip was subjected to a regeneration pulse (30 s with 10 mM glycine-HCl at pH 1.5) followed by a stabilization period (30 s) and, finally, a buffer injection (60 s) to verify the mass transfer effect.

Binding assays were assessed in real-time by a sensorgram of association and dissociation for the complex formation, and changes in the SPR angle were expressed as resonance units (RU) using the Qdat software (version 4.3.1, FortéBio, New York, NY, USA). To avoid artifacts, RU values from the reference channel were subtracted from the RU values of the test samples. The rate constants that measure interactions between proteins–drugs can be expressed as an association rate constant (k_a or k_{on}) and/or a dissociation rate constant (k_d or k_{off}), which are used to determine the equilibrium or affinity constant (K_D; Equation (2)) [36]. Thus, K_D was the nomenclature adopted in this work to define affinity.

$$K_D = \frac{k_a}{k_d} \quad (2)$$

3. Results and Discussion

3.1. Identification of the Main Fluorescence Quenching Mechanism

According to Soares and coworkers [30], the bimolecular quenching rate constant (k_q) values for the interaction of HSA/HCTZ in nonglycemic, normoglycemic, or hyperglycemic conditions are in the order of 10^{12} M^{-1} s^{-1}, larger than the diffusion rate constant in water (k_{diff}~7.40×10^9 M^{-1} s^{-1} at 298 K, following the Smoluchowski–Stokes–Einstein theory) [37], indicating a ground state association. However, in the Stern–Volmer plot, we noticed the appearance of a negative curvature at the highest glucose level (320 mg/dL), which was not expected in a pure static quenching mechanism [31]. Thus, to clarify the

fluorescence quenching mechanism operating in the HSA/HCTZ complex, time-resolved fluorescence measurements were conducted in the absence and presence of the maximum HCTZ concentration used in the reported steady-state fluorescence analysis [30] (Figure 2 and Table 1).

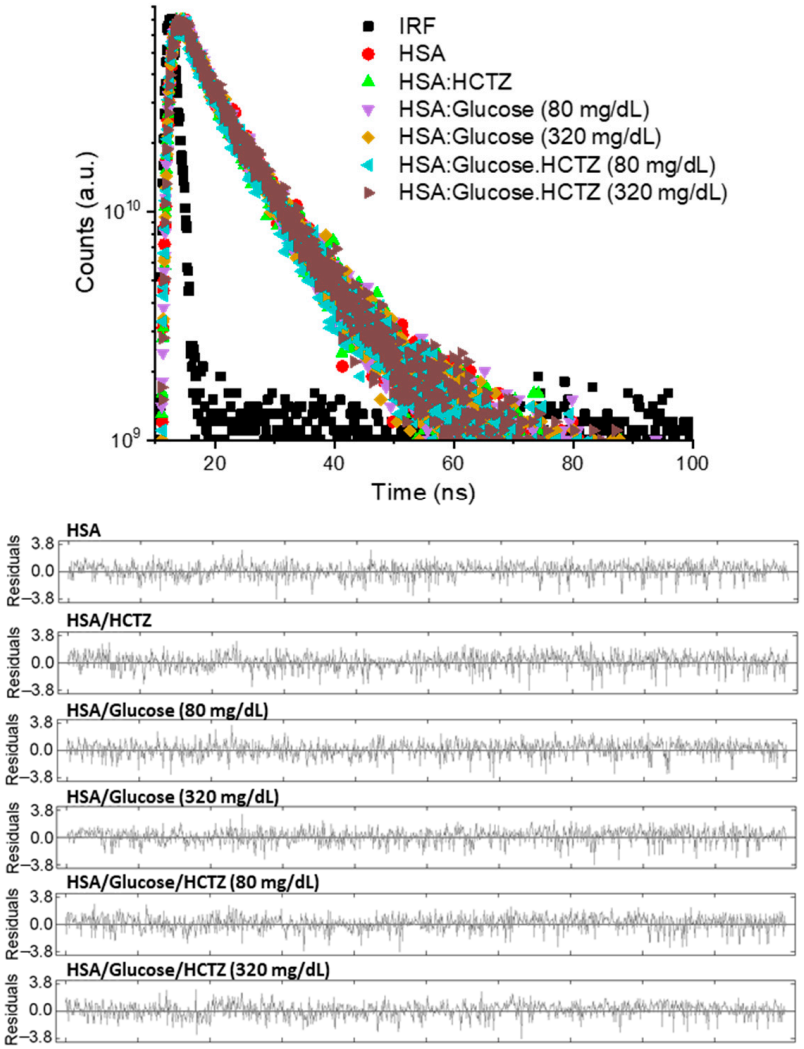


Figure 2. Time-resolved fluorescence decays for HSA (10 μM) in nonglycemic, normoglycemic (80 mg/dL), and hyperglycemic (320 mg/dL) conditions without and in the presence of HCTZ (13.4 μM) at room temperature.

Table 1. Time-resolved fluorescence parameters for HSA, HSA/HCTZ, HSA/glucose, and HSA/glucose/HCTZ in a PBS solution (pH 7.4) at room temperature.

System	τ_1 (ns)	%Relative	τ_2 (ns)	% Relative	$\tau_{average}$ (ns)	χ^2
HSA	1.76 ± 0.09	24.8	5.75 ± 0.09	75.2	4.76	1.158
HSA/HCTZ	1.69 ± 0.09	25.1	5.66 ± 0.09	74.9	4.66	1.125
HSA/glucose (80 mg/dL)	1.73 ± 0.10	23.2	5.65 ± 0.09	76.8	4.74	1.115
HSA/glucose (320 mg/dL)	1.71 ± 0.09	23.9	5.73 ± 0.09	76.1	4.77	1.191
HSA/glucose/HCTZ (80 mg/dL)	1.75 ± 0.09	25.5	5.74 ± 0.09	74.5	4.72	1.154
HSA/glucose/HCTZ (320 mg/dL)	1.71 ± 0.10	22.1	5.59 ± 0.09	77.9	4.73	1.193

The fluorescence decays were better fitted in a bi-exponential function (residuals in Figure 2), with the measured corresponding shorter (τ_1) and longer lifetimes (τ_2) for non-bound HSA in a nonglycemic condition of 1.76 ± 0.09 and 5.75 ± 0.09 ns, in full agreement with the literature data [38,39]. Since the fluorescence lifetimes for HSA did not significantly change in the presence of HCTZ, it can be stated that the quenching process occurred through a purely static mechanism [31], indicating that the Stern–Volmer technique, and not the double-logarithmic approach, is the best mathematical approximation to estimate the binding affinity of HSA/HCTZ [40,41]. Thus, the reported Stern–Volmer quenching constant (K_{sv}), and not the apparent binding constant (K_b), must be considered to estimate the binding affinity of albumin/HCTZ, correcting the approach carried out by Soares and coworkers [30]. In this sense, the reported K_{sv} value of (1.38 ± 0.01) × 10^4 M^{-1} at 310 K [30] indicated a moderate binding affinity.

Glucose in both normoglycemic and hyperglycemic concentrations in the HSA solution did not significantly decrease the lifetimes of albumin (Table 1), agreeing with previous trends reported for different monosaccharides [20]. The interaction of HSA/HCTZ in normoglycemic and hyperglycemic conditions decreased albumin's average fluorescence lifetime by less than 1% (Table 1), indicating that under the two different glucose levels used in this work, the fluorescence quenching mechanism induced by HCTZ continues to be purely static. Energy transfer (from the dynamic quenching mechanism) does not operate in the system under study. Thus, even in the presence of glucose, HCTZ still might interact via a ground state association, and the reported K_{SV} values of 1.57 ± 0.03 and 2.82 ± 0.09 × 10^4 M^{-1} for normoglycemic and hyperglycemic conditions, respectively, [30] indicate that these glucose levels might increase HCTZ's affinity to albumin, increasing by about two-fold at extreme glucose concentrations.

It is important to highlight that high glucose levels cause oxidative changes in proteins (glycoxidation), inducing the formation of Maillard reaction products and further advanced glycation end-products [42]. Thus, glycoxidation in patients with diabetes under long exposure to high glucose concentrations in the blood is feasible, leading to the formation of glycated albumin [43]. Under the experimental in vitro conditions used in this work, we did not induce the glycoxidation of albumin. We did not identify any significant change in the τ values for HSA and HSA/glucose that could indicate glycoxidation [44,45].

3.2. STD-NMR Analysis

To deeply evaluate the binding mode of HCTZ with HSA, we performed STD-NMR experiments. The STD-NMR technique enables the identification of the binding epitope on the ligand by assessing the efficiency of saturation transfer from the specifically saturated protein. The saturation transfer efficiency is quantitatively expressed by the amplification factor (A_{STD}), representing the average number of transient contacts of the ligand per molecule of the receptor within a given saturation time [33]. The A_{STD} plot obtained for HCTZ (Figure 3) depicts that for the three observable hydrogens in HCTZ's structure (H3, H7, and H10), H10 exhibited a stronger A_{STD} than H7 (100% vs. 67.1%, respectively) while no signal corresponding to H3 was observed in the on-resonance spectrum. Thus, the STD percentage data indicate that H10 is closer than H7 to the amino acid residues of albumin, and H3 is the most distant from the binding site, contributing to a comprehensive understanding of the interaction of albumin/HCTZ.

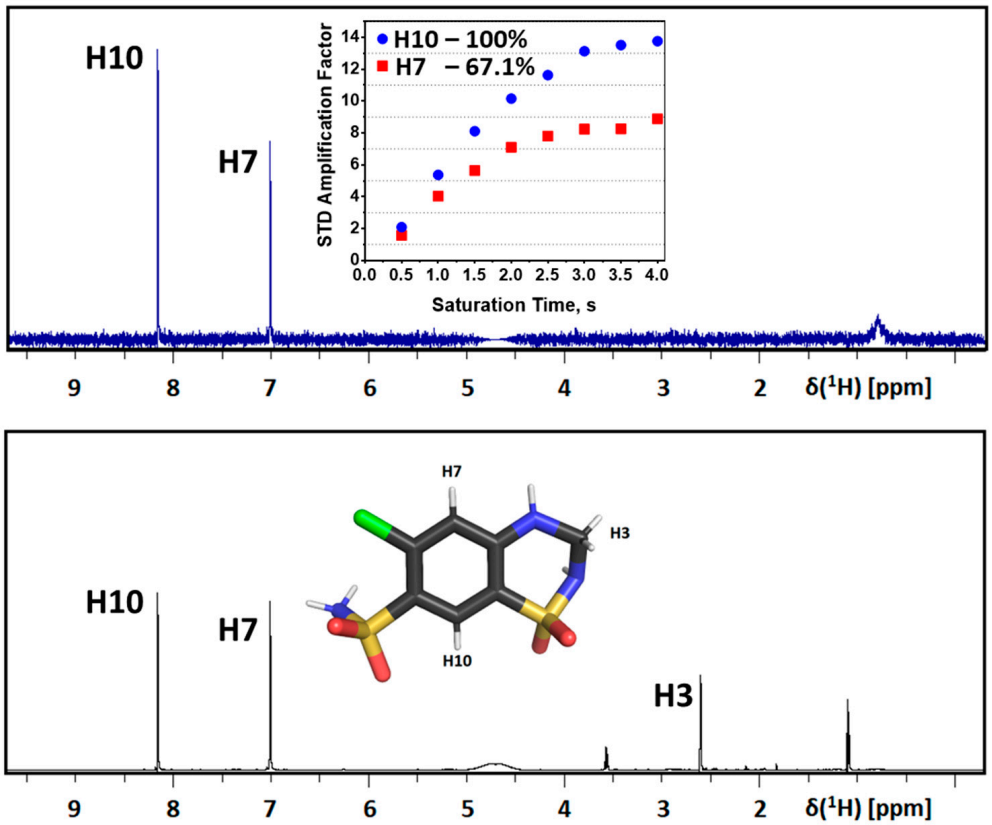


Figure 3. Analysis of STD-NMR reveals the binding epitope of HCTZ in HSA protein in nonglycemic conditions. The reference spectrum acquired in the off-resonance condition is depicted in black, while the corresponding STD-NMR spectrum is presented in blue. The chemical structure of HCTZ featuring assigned protons is illustrated as an inset in the reference spectrum. The STD amplification factor is plotted as a function of the saturation time, accompanied by the estimated relative STD percentages for each HCTZ signal. Elements' color: Chlorine, oxygen, nitrogen, sulfur, and carbon in green, red, blue, yellow, and black, respectively.

To contribute to the evaluation of glucose's effect on the interaction of HSA/HCTZ, we conducted STD-NMR experiments on HCTZ in the presence of increasing concentrations of glucose. In this case, we did not observe any evidence of glucose binding in HSA, even with the highest concentration of glucose (20 mM), which gave a 1000-fold ligand excess compared with the protein (Figure 4A–C). From the literature, it is known that glucose might interact with albumin very weakly with a binding constant of 10^2 M^{-1} [20,46], and, probably for this reason, the STD-NMR results did not detect the complex of HSA/glucose. Moreover, the presence of glucose in an equimolar proportion of HCTZ did not affect the binding of the drug to albumin. There was not any significant alteration in the amplification factor of HCTZ signals in the mixture (Figure 4D). In the concentrations of glucose five- and ten-fold higher than the drug, the interaction of HSA/HCTZ (Figure 4B,C) was still observed with an improvement in the A_{STD} (Figure 4D), indicating that glucose in concentrations higher than those of HCTZ might increase the binding capacity of this drug to albumin, agreeing with the time-resolved fluorescence results.

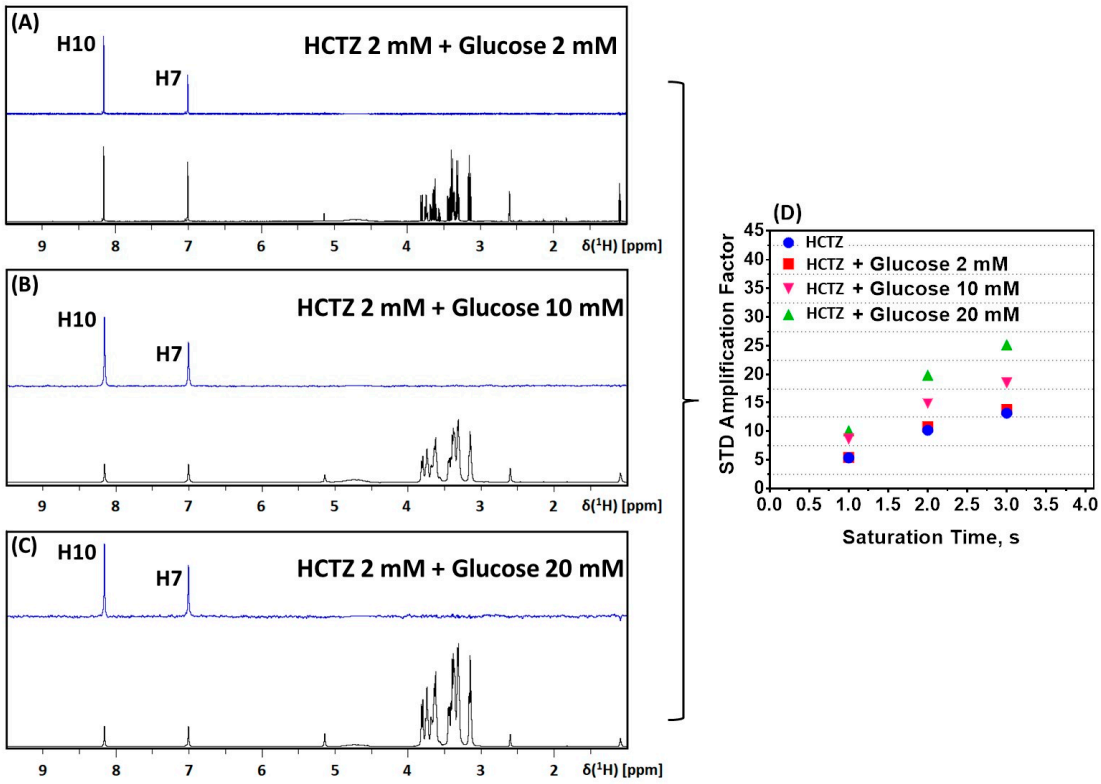


Figure 4. STD-NMR experiments on HCTZ with increasing concentrations of glucose: (**A**) 2 mM, (**B**) 10 mM, and (**C**) 20 mM. The reference spectrum acquired for each glucose concentration is given in black (off-resonance), and the corresponding STD-NMR spectrum is colored in blue. (**D**) A_{STD} plot of HCTZ in the presence and absence of glucose.

Overall, the new interpretation of the reported K_{SV} values [30] based on the obtained time-resolved fluorescence and STD-NMR data indicates that high glucose levels significantly increase the binding capacity of HCTZ to albumin, indicating the importance of glycemic control in the human bloodstream to obtain the appropriate residence time and pharmacotherapeutic treatment for the commercial drug HCTZ.

3.3. SPR Analysis

Balaei and Ghobadi [47] detected the interaction of albumin/HCTZ in subdomain IIA (the warfarin-binding site, site I) and not in subdomain IIIA (the ibuprofen-binding site, site II); however, they did not explore the possibility of interaction with subdomain IB (the digitoxin-binding site), a newly discovered binding region that, due to its importance in albumin–drugs interactions, is considered site III [48]. Since both time-resolved fluorescence and STD-NMR experiments indicated an improvement in the binding capacity of HCTZ with glucose, positive cooperativity was expected to increase the drug interaction with subdomain IIA or with other subdomains, e.g., IB. Site III can be considered a feasible binding site for HCTZ due to its high positive electrostatic potential region like site I [21,49]. Thus, SPR experiments were performed without and in the presence of the site markers warfarin or digitoxin to provide the binding property of HCTZ to subdomains IIA and IB.

The binding of HSA to the sensor chip exhibited a significant binding rate of 8000 resonance units per second (RU/s). Therefore, the HSA binding site was accessible to interactions with specific ligands in the solution. The variation in RU/s time over 200 s was used to evaluate the interactions between HSA and HCTZ, warfarin, and digitoxin (Figure 5A). The site markers (warfarin and digitoxin) and the antihypertensive drug were further analyzed using a series of concentrations, which demonstrated an increase in

SPR signals (RU/s), indicating a direct binding to immobilized HSA in a concentration-dependent manner (R^2 = 0.99 for all tests; Figure 5B).

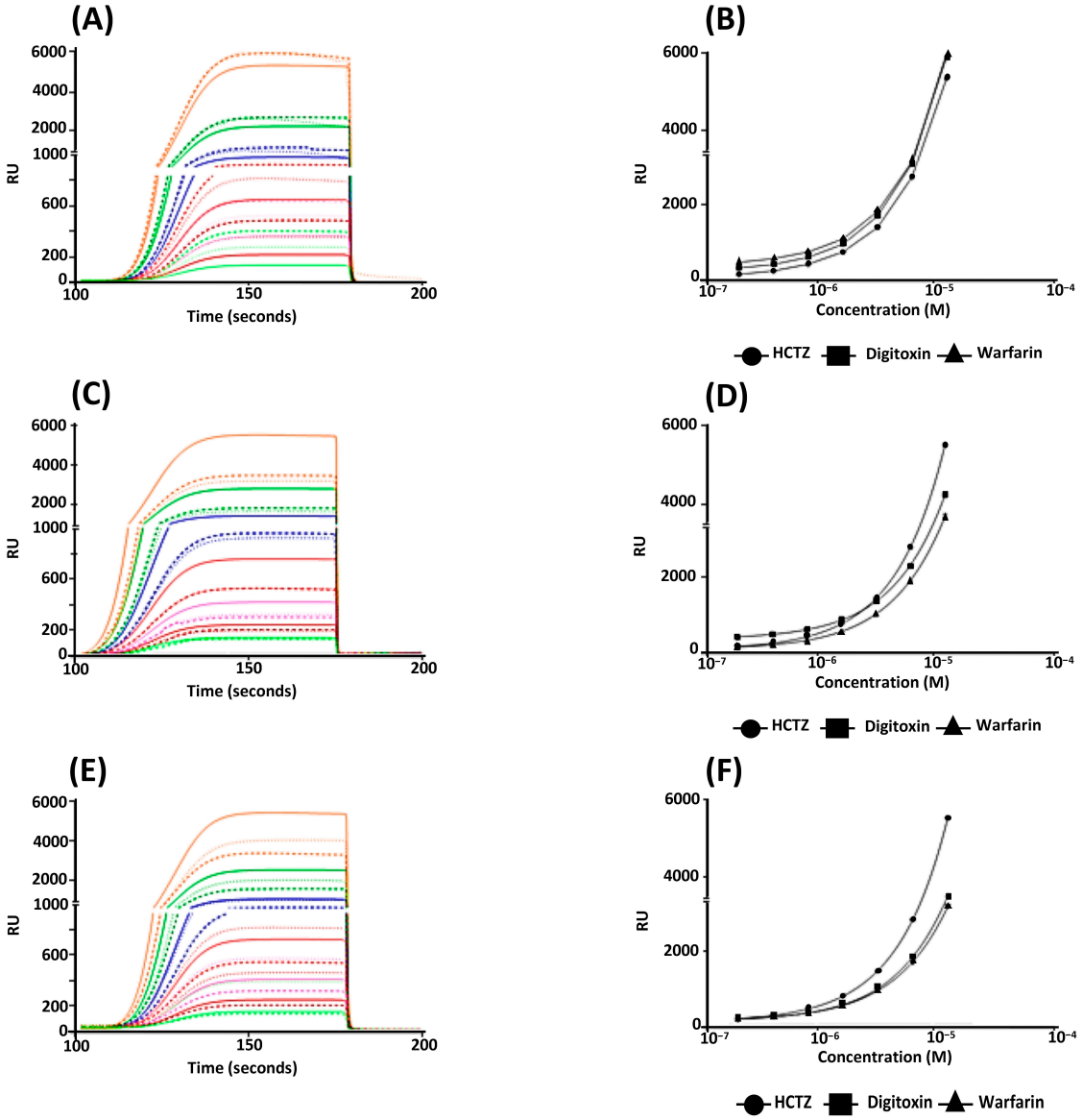


Figure 5. SPR assays assessing the interactions between the HSA and some specific ligands. These experiments were performed with HSA on a COOH5 chip. (**A**,**B**) Accessing the bioavailability of multiple HSA binding sites after immobilization onto the sensor chip by using warfarin, HCTZ, and digitoxin. (**C**,**D**) Inhibition assays of (i) HSA binding to HCTZ without inhibitor (wi) and in the presence of warfarin or digitoxin. (**E**,**F**) Competition assays of HCTZ binding to HSA in nonglycemic, normoglycemic (80 mg/dL), and hyperglycemic (320 mg/dL) conditions. (**A**,**C**,**E**) Data are presented as average sensorgrams (resonance signal versus time, representative of three independent experiments) and (**B**,**D**,**F**) nonlinear regression curve fit (the error bars represent a standard deviation of approximately 1.0% of the average value, rendering them barely visible in the graphs); 1.34×10^{-5} M (■), 6.70×10^{-6} M (■), 3.35×10^{-6} M (■), 1.68×10^{-6} M (■), 8.38×10^{-7} M (■), 4.19×10^{-7} M (■), and 2.09×10^{-7} M (■).

The binding affinities between HSA and the three specific ligands were evaluated by the affinity constant (K_D; Table 2). The obtained results showed the bioavailability of multiple HSA binding sites after immobilization on the sensor chip, which was confirmed due to the different K_D values for warfarin, digitoxin, and HCTZ. The obtained K_D values

for the site markers were in the same order of magnitude as those previously reported in the literature [50,51]. The K_D value for HCTZ under the nonglycemic condition was comparable to the reported K_{SV} value in [30], indicating the reliability of the new approach obtained by time-resolved fluorescence measurements (Section 3.1). Competitive binding studies were performed in the presence of the site markers warfarin and digitoxin. There was a higher inhibition of HCTZ binding in the presence of warfarin than digitoxin on the HSA after immobilization on the sensor chip. Furthermore, it was possible to verify that digitoxin can affect drug binding at a concentration of 0.67 μM (Figure 5C,D). These results indicate that subdomain IIA is the main binding site of HCTZ to albumin; however, subdomain IB can also accommodate HCTZ but to a lesser extent, corroborating the previous discussion (Section 3.2) about more than one feasible binding site. This trend was not previously detected by Balaei and Ghobadi [47] due to the lack of drug-displacement assays for subdomain IB.

Table 2. Binding affinity values ($K_D \times 10^{-6}$ M) of the interactions between HSA and drugs.

Binding Sites Biodisponibility			**Inhibition of HCTZ Binding in Presence of:**		**Competition with HCTZ Binding**	
HCTZ	Digitoxin	Warfarin	Digitoxin	Warfarin	Normoglycemic	Hyperglycemic
180.0 ± 40	78.0 ± 4.0	37.0 ± 1.0	22.9 ± 0.6	62.0 ± 4.0	218.0 ± 6.0	114.0 ± 2.0

The binding profile of HCTZ with HSA under glucose-enriched conditions was also evaluated (Figure 5E,F). The results suggest that glucose in the SPR running buffer can affect the affinity of HCTZ for albumin mainly in the hyperglycemic condition, i.e., the K_D value in the hyperglycemic condition decreased by about 1.6-fold compared with the normoglycemic condition (Table 2). This result agrees with recent research that indicates the presence of glucose influences the drug–albumin interaction via cooperativity and/or perturbation in the albumin structure, which induces the protein's pockets to receive drugs [29].

4. Conclusions

The time-resolved fluorescence analysis for HSA/HCTZ indicated that the fluorescence lifetime average did not significantly change in both nonglycemic, normoglycemic, and hyperglycemic conditions. Thus, a purely static quenching mechanism is operating, which results in a ground-state association close to the fluorophore Trp-214 residue (subdomain II). Thus, the reported K_{SV} value is the best constant via fluorescence to estimate the binding affinity—moderate. The SPR results agreed with the time-resolved fluorescence data, indicating subdomain IIA as the main binding site; however, there is the possibility of subdomain IB also being considered as a secondary binding site, mainly in the hyperglycemic condition, due to the cooperativity and/or perturbations in the protein's structure. Finally, both the time-resolved fluorescence and STD-NMR results showed that even in the presence of different levels of glucose, HCTZ continuously interacted with albumin, indicating that glucose under hyperglycemic conditions led the cavities to be more likely to receive more ligands. Thus, there is a necessity for glucose control in the human bloodstream to not impact the residence time (pharmacokinetic profile) and pharmacotherapeutic potential of HCTZ.

Author Contributions: Conceptualization, O.A.C.; methodology, C.R.A., L.V. and O.A.C.; validation, C.S. and O.A.C.; formal analysis, M.A.G.S., F.S.-S., L.V., T.S.d.A. and O.A.C.; investigation, M.A.G.S., F.S.-S., C.R.A., T.S.d.A., C.S. and O.A.C.; resources, C.S. and O.A.C.; data curation, O.A.C.; writing—original draft preparation, M.A.G.S., F.S.-S., C.R.A., T.S.d.A. and O.A.C.; writing—review and editing, L.V., C.S. and O.A.C.; visualization, O.A.C.; supervision, O.A.C.; project administration, O.A.C.; funding acquisition, C.R.A. and C.S. All authors have read and agreed to the published version of the manuscript.

Funding: This research was funded by the following Brazilian agencies: Conselho Nacional de Desenvolvimento Científico e Tecnológico (CNPq: 301744/2019-0), Coordenação de Aperfeiçoamento de Pessoal de Nível Superior (CAPES: 001), and Fundação de Amparo à Pesquisa do Estado do Rio de Janeiro (FAPERJ: E-26/200.799/2021). Carlos R. Alves is a research fellow at CNPq. Franklin Souza-Silva is a research fellow at CAPES. Additionally, the authors acknowledge the Coimbra Chemistry Centre that is supported by the Fundação para a Ciência e a Tecnologia (FCT—the Portuguese Agency for Scientific Research) through the projects UIDB/00313/2020 and UIDP/00313/2020. Otávio Augusto Chaves thanks the FCT for his Ph.D. fellowship 2020.07504.BD (https://doi.org/10.54499/2020.07504.BD, accessed on 1 February 2024).

Institutional Review Board Statement: Not applicable.

Informed Consent Statement: Not applicable.

Data Availability Statement: The data are contained within this article.

Acknowledgments: The authors thank the technical support from the Nanotechnology Platform (subunit RPT03E-IOC) of the Oswaldo Cruz Foundation and the Oswaldo Cruz Institute, especially Luzia Monteiro de Castro-Côrtes.

Conflicts of Interest: The authors declare no conflicts of interest.

References

1. Mansur, A.P.; Favarato, D. Mortality due to cardiovascular diseases in Brazil and in the metropolitan region of São Paulo: A 2011 update. *Arq. Bras. Cardiol.* **2012**, *99*, 755–761. [CrossRef] [PubMed]
2. Chang, K.Y.; Duval, S.; Badesch, D.B.; Bull, T.M.; Chakinala, M.M.; de Marco, T.; Frantz, R.P.; Hemnes, A.; Mathai, S.C.; Rosenzweig, E.B.; et al. Mortality in pulmonary arterial hypertension in the modern era: Early insights from the pulmonary hypertension association registry. *J. Am. Heart Assoc.* **2022**, *11*, e024969. [CrossRef] [PubMed]
3. Nascimento, B.R.; Brant, L.C.C.; Oliveira, G.M.M.; Malachias, M.V.B.; Reis, G.M.A.; Teixeira, R.A.; Malta, D.C.; França, E.; Souza, M.F.M.; Roth, G.A.; et al. Cardiovascular disease epidemiology in Portuguese-speaking countries: Data from the global burden of disease, 1990 to 2016. *Arq. Bras. Cardiol.* **2018**, *110*, 500–511. [CrossRef] [PubMed]
4. Boateng, E.B.; Ampofo, A.G. A glimpse into the future: Modelling global prevalence of hypertension. *BMC Public Health* **2023**, *23*, 1906. [CrossRef] [PubMed]
5. Amini, M.; Zayeri, F.; Salehi, M. Trend analysis of cardiovascular disease mortality, incidence, and mortality-to-incidence ratio: Results from global burden of disease study 2017. *BMC Public Health* **2021**, *21*, 401. [CrossRef] [PubMed]
6. NCD Risk Factor Collaboration (NCD-RisC). Worldwide trends in hypertension prevalence and progress in treatment and control from 1990 to 2019: A pooled analysis of 1201 population-representative studies with 104 million participants. *Lancet* **2021**, *398*, 957–980. [CrossRef] [PubMed]
7. Lira, A.; Cláudia, M.; de Souza, M.; Mayara, N.; Burgos, P.A.; Goretti, M. Prevalência de fatores de risco para doenças cardiovasculares em diabéticas. *Nutr. Clín. Diet. Hosp.* **2017**, *37*, 75–81.
8. Siqueira, A.F.A.; Almeida-Pititto, B.; Ferreira, S.R.G. Cardiovascular disease in diabetes mellitus: Classical and non-classical risk factors. *Arq. Bras. Endocrinol. Metab.* **2017**, *51*, 257–267. [CrossRef] [PubMed]
9. Leon, B.M.; Maddox, T.M. Diabetes and cardiovascular disease: Epidemiology, biological mechanisms, treatment recommendations and future research. *World J. Diabetes* **2015**, *6*, 1246–1258. [CrossRef]
10. Chanda, R.; Fenves, A.Z. Hypertension in patients with chronic kidney disease. *Curr. Hypertens. Rep.* **2009**, *11*, 329–336. [CrossRef]
11. Yeates, K.; Lohfeld, L.; Sleeth, J.; Morales, F.; Rajkotia, Y.; Ogedegbe, O. A global perspective on cardiovascular disease in vulnerable populations. *Can. J. Cardiol.* **2015**, *31*, 1081–1093. [CrossRef] [PubMed]
12. Krum, H.; Skiba, M.; Gilbert, R.E. Comparative metabolic effects of hydrochlorothiazide and indapamide in hypertensive diabetic patients. *Diabet. Med.* **2003**, *20*, 708–712. [CrossRef] [PubMed]
13. Bertoluci, M.C.; Pimazoni-Netto, A.; Pires, A.C.; Pesaro, A.E.; Schaan, B.D.; Caramelli, B.; Polanczyk, C.A.; Júnior, C.V.S.; Gualandro, D.M.; Malerbi, D.A.; et al. Diabetes and cardiovascular disease: From evidence to clinical practice–position statement 2014 of Brazilian Diabetes Society. *Diabetol. Metab. Syndr.* **2014**, *20*, 58. [CrossRef] [PubMed]
14. Mancia, G.; Kreutz, R.; Brunstrom, M.; Burnier, M.; Grassi, G.; Januszewicz, A.; Muiesan, M.L.; Tsioufis, K.; Agabiti-Rosei, E.; Algharably, E.A.E.; et al. 2023 ESH Guidelines for the management of arterial hypertension The Task Force for the management of arterial hypertension of the European Society of Hypertension: Endorsed by the International Society of Hypertension (ISH) and the European Renal Association (ERA). *J. Hypertens.* **2023**, *41*, 1874–2071. [PubMed]
15. Williams, B.; Mancia, G.; Spiering, W.; Rosei, E.A.; Azizi, M.; Burnier, M.; Clement, D.L.; Coca, A.; de Simone, G.; Dominiczak, A.; et al. 2018 ESC/ESH Guidelines for the management of arterial hypertension: The Task Force for the management of arterial hypertension of the European Society of Cardiology (ESC) and the European Society of Hypertension (ESH). *Europ. Heart J.* **2018**, *39*, 3021–3104. [CrossRef] [PubMed]

16. Moreira, M.L.S.; Chaves, O.A.; de Lucas, N.C.; Goulart, J.S.; Garden, S.J.; Serpa, C.; Netto-Ferreira, J.C. Spectroscopic and in silico characterization of the interaction between synthetic 2-substituted-naphtho-1,4-quinones and human serum albumin. *J. Mol. Liq.* **2024**, *403*, 124829. [CrossRef]
17. Mukai, R.; Okuyama, H.; Uchimura, M.; Sakao, K.; Matsuhiro, M.; Ikeda-Imafuku, M.; Ishima, Y.; Nishikawa, M.; Ikushiro, S.; Tai, A. The binding selectivity of quercetin and its structure-related polyphenols to human serum albumin using a fluorescent dye cocktail for multiplex drug-site mapping. *Bioorg. Chem.* **2024**, *145*, 107184. [CrossRef] [PubMed]
18. Sargolzaei, J.; Jalali, E.; Rajabi, P. Insights into the binding of buspirone to human serum albumin using multi-spectroscopic and molecular docking techniques. *Heliyon* **2024**, *8*, e29430. [CrossRef] [PubMed]
19. Yang, Y.; Hu, J.; Wang, H.; Qiao, L.; Wang, Y.; Tong, W.; Zhao, L. Deciphering the binding mechanisms of eugenol and 2-methylpyrazine with human serum albumin using technical approach. *J. Mol. Liq.* **2024**, *405*, 124981. [CrossRef]
20. Chaves, O.A.; Soares, M.A.G.; Oliveira, M.C.C. Monosaccharides interact weakly with human serum albumin. Insights for the functional perturbations on the binding capacity of albumin. *Carbohydr. Res.* **2021**, *501*, 1082742. [CrossRef]
21. Costa-Tuna, A.; Chaves, O.A.; Loureiro, R.J.S.; Pinto, S.; Pina, J.; Serpa, C. Interaction between a water-soluble anionic porphyrin and human serum albumin unexpectedly stimulates the aggregation of the photosensitizer at the surface of the albumin. *Int. J. Biol. Macromol.* **2024**, *225*, 128210. [CrossRef] [PubMed]
22. Jalali, E.; Sargolzaei, J.; Rajabi, P. Investigating the interaction between sertraline hydrochloride and human serum albumin using equilibrium dialysis and spectroscopic methods. *Inorg. Chem. Commun.* **2024**, *166*, 112586. [CrossRef]
23. Sliwinska-Hill, U.; Krzyzak, E.; Czyznikowska, Z. The effect of simultaneous binding of doxorubicin and cyclophosphamide on the human serum albumin structure. *J. Mol. Liq.* **2024**, *404*, 125003. [CrossRef]
24. Akbari, V.; Ghobadi, S. Evaluation of the effect of phenylpropanoids on the binding of heparin to human serum albumin and glycosylated human serum albumin concerning anticoagulant activity: A comparison study. *Int. J. Biol. Macromol.* **2024**, *257*, 128732. [CrossRef]
25. Rodrigues, B.M.; Victória, H.F.V.; Leite, G.; Krambrock, K.; Chaves, O.A.; de Oliveira, R.Q.; de Boni, L.; Costa, L.A.S.; Iglesias, B.A. Photophysical, photobiological, and biomolecule-binding properties of new tri-cationic meso-tri(2-thienyl)corroles with Pt(II) and Pd(II) polypyridyl derivatives. *J. Inorg. Biochem.* **2023**, *242*, 112149. [CrossRef] [PubMed]
26. Chaves, O.A.; Loureiro, R.J.S.; Costa-Tuna, A.; Almeida, Z.L.; Pina, J.; Brito, R.M.M.; Serpa, C. Interaction of two comercial azobenzene food dyes, amaranth and new coccine, with human serum albumin: Biophysical characterization. *ACS Food Sci. Technol.* **2023**, *3*, 955–968. [CrossRef]
27. Hu, X.; Wang, J.-Z.; Liu, Q.-H.; Ding, X.; Yin, M.-M.; Hu, Y.-J. Bisphenol a modification and how its structure influences human serum albumin binding force. *J. Mol. Liq.* **2024**, *401*, 124655. [CrossRef]
28. Raghav, A.; Ahmad, J.; Alam, K. Nonenzymatic glycosylation of human serum albumin and its effect on antibodies profile in patients with diabetes mellitus. *PLoS ONE* **2017**, *12*, e0176970. [CrossRef] [PubMed]
29. Soares, M.A.G.; de Aquino, P.A.; Costa, T.; Serpa, C.; Chaves, O.A. Insights into the effect of glucose on the binding between human serum albumin and the nonsteroidal anti-inflammatory drug nimesulide. *Int. J. Biol. Macromol.* **2024**, *265*, 131148. [CrossRef]
30. Soares, M.A.G.; Chaves, O.A.; Cesarin-Sobrinho, D.; Silva, D.; Cortez, C.M. Effect of blood glucose levels on the HSA-hydrochlorothiazide interaction—A spectrofluorimetric study. *Int. J. Health Sc.* **2021**, *1*, 1–17. [CrossRef]
31. Lakowicz, J.R. *Principles of Fluorescence Spectroscopy*, 3rd ed.; Springer: Boston, MA, USA, 2006.
32. Walpole, S.; Monaco, S.; Nepravishta, R.; Ângulo, J. STD NMR as a technique for ligand screening and structural studies. *Methods Enzymol.* **2019**, *615*, 423–451. [PubMed]
33. Viegas, A.; Manso, J.; Nobrega, F.L.; Cabrita, E.J. Saturation-transfer difference (STD) NMR: A simple and fast method for ligand screening and characterization of protein binding. *J. Chem. Ed.* **2011**, *88*, 990–994. [CrossRef]
34. Santos-de-Souza, R.; Souza-Silva, F.; de Albuquerque-Melo, B.C.; Ribeiro-Guimarães, M.L.; Côrtes, L.M.C.; Pereira, B.A.S.; Silva-Almeida, M.; Cysne-Finkelstein, L.; Junior, F.O.R.O.; Pereira, M.C.S.; et al. Insights into the tracking of the cysteine proteinase B COOH-terminal polypeptide of Leishmania (Leishmania) amazonensis by surface plasmon resonance. *Parasitol. Res.* **2019**, *118*, 1249–1259. [CrossRef] [PubMed]
35. Vachali, P.; Li, B.; Nelson, K.; Bernstein, P.S. Surface plasmon resonance (SPR) studies on the interactions of carotenoids and their binding proteins. *Ach. Biochem. Biophys.* **2012**, *519*, 32–47. [CrossRef] [PubMed]
36. Jarmoskaite, I.; AlSadhan, I.; Vaidyanathan, P.P.; Herschlag, D. How to measure and evaluate binding affinities. *eLife* **2020**, *9*, e57264. [CrossRef] [PubMed]
37. Montalti, M.; Credi, A.; Prodi, L.; Gandolfi, M.T. *Handbook of Photochemistry*, 3rd ed.; CRC Press: Boca Raton, FL, USA, 2006.
38. Bai, G.; Cui, Y.; Yang, Y.; Ye, C.; Liu, M. A competitive low-affinity binding model for determining the mutual and specific sites of two ligands on protein. *J. Pharm. Biomed. Anal.* **2005**, *38*, 588–593. [CrossRef] [PubMed]
39. Liu, Y.; Yuan, Z.; Zhao, P.; Li, C.; Qin, L.; Zhao, T.; Zhu, X.; Feng, S. Studies on the binding of wedelolactone to human serum albumin with multi-spectroscopic analysis, molecular docking and molecular dynamic simulation. *Biophys. Chem.* **2024**, *307*, 107198. [CrossRef] [PubMed]
40. Moreno, M.J.; Loura, L.M.S.; Martins, J.; Salvador, A.; Velazquez-Campoy, A. Analysis of the equilibrium distribution of ligands in heterogeneous media–Approaches and pitfalls. *Int. J. Mol. Sci.* **2022**, *23*, 9757. [CrossRef] [PubMed]

41. Costa-Tuna, A.; Chaves, O.A.; Almeida, Z.L.; Cunha, R.S.; Pina, J.; Serpa, C. Profiling the interaction between human serum albumin and clinically relevant HIV reverse transcriptase inhibitors. *Viruses* **2024**, *16*, 491. [CrossRef]
42. Rondeau, P.; Bourdon, E. The glycation of albumin: Structural and functional impacts. *Biochimie* **2011**, *93*, 645–658. [CrossRef]
43. Arasteh, A.; Farahi, S.; Habibi-Rezaei, M.; Moosavi-Movahedi, A.A. Glycated albumin: An overview of the In Vitro models of an In Vivo potential disease marker. *J. Diabetes Metab. Disord.* **2014**, *13*, 49. [CrossRef] [PubMed]
44. Sadowska-Bartosz, I.; Galiniak, S.; Bartosz, G. Kinetics of glycoxidation of bovine serum albumin by glucose, fructose and ribose and its prevention by food components. *Molecules* **2014**, *19*, 18828–18849. [CrossRef]
45. Wybranowski, T.; Ziomkowska, B.; Cyrankiewicz, M.; Bosek, M.; Pyskir, J.; Napiórkoska, M.; Kruszewski, S. A study of the oxidative processes in human plasma by time-resolved fluorescence spectroscopy. *Sci. Rep.* **2022**, *12*, 9012. [CrossRef] [PubMed]
46. Wang, Y.; Yu, H.; Shi, X.; Luo, Z.; Lin, D.; Huang, M. Structural mechanism of ring-opening reaction of glucose by human serum albumin. *J. Biol. Chem.* **2013**, *288*, 15980–15987. [CrossRef] [PubMed]
47. Balaei, F.; Ghobadi, S. Hydrochlorothiazide binding to human serum albumin induces some compactness in the molecular structure of the protein: A multi-spectroscopic and computational study. *J. Pharm. Biomed. Anal.* **2019**, *162*, 1–8. [CrossRef] [PubMed]
48. Hage, D.S.; Sengupta, A. Characterisation of the binding of digitoxin and acetyldigitoxin to human serum albumin by high-performance affinity chromatography. *J. Chromatogr. B Biomed. Appl.* **1999**, *724*, 91–100. [CrossRef] [PubMed]
49. Chaves, O.A.; Iglesias, B.A.; Serpa, C. Biophysical characterization of the interaction between a transport human plasma protein and the 5,10,15,20-tetra(pyridine-4-yl)porphyrin. *Molecules* **2022**, *27*, 5341. [CrossRef] [PubMed]
50. Eskew, M.W.; Benight, A.S. Ligand binding constants for human serum albumin evaluated by ratiometric analysis of DSC thermograms. *Anal. Biochem.* **2021**, *628*, 114293. [CrossRef]
51. Rich, R.L.; Day, Y.S.; Morton, T.A.; Myszka, D.G. High-resolution and high-throughput protocols for measuring drug/human serum albumin interactions using BIACORE. *Anal. Biochem.* **2001**, *296*, 197–207. [CrossRef]

Disclaimer/Publisher's Note: The statements, opinions and data contained in all publications are solely those of the individual author(s) and contributor(s) and not of MDPI and/or the editor(s). MDPI and/or the editor(s) disclaim responsibility for any injury to people or property resulting from any ideas, methods, instructions or products referred to in the content.